J. Am. Chem. Soc. **2001,** *123,* 545−553

Kinetic Resolution Using Enantioimpure Catalysts: Mechanistic Considerations of Complex Rate Laws

Donna G. Blackmond*

Contribution from the Department of Chemistry, University of Hull, Hull HU6 7RX, United Kingdom

Received July 13, 2000

Abstract: Kinetic resolutions in which the reactions exhibit complex rate laws are discussed. When enantioimpure catalysts are employed, a conversion-dependent selectivity factor k_{rel} may in some cases be observed due to "kinetic partitioning" of catalysts within a reaction network. Both asymmetric amplifications and depletions may be observed, and the effects are separate from—and may in some cases be superimposed on—the classic nonlinear effect due to catalyst interactions as those predicted by Kagan's ML_n models. Consideration of the conversion dependence of the selectivity factor using enantioimpure catalysts reveals significant detail about the reaction mechanism for the enantiopure case and may offer insights for practical application of kinetic resolution. Examples from the literature are analyzed in the context of kinetic partitioning.

Introduction

Kinetic resolutions represent an efficient method for producing enantiopure compounds, and both enzymatic and nonenzymatic resolution processes have been extensively studied and reviewed.[1] The principle of kinetic resolution rests on a difference in the rate of transformation of the enantiomers in a racemic or enantioimpure substrate mixture so that the substrate enantiopurity increases with conversion. The reaction product may itself be either chiral or achiral. Mathematical expressions have been developed describing the efficiency of the process in terms of the concentration dependence of reaction rate for the two enantiomeric substrates and a selectivity factor k_{rel}, (eq 1).[1] For simple first- and second-order kinetics in substrate concentration, analytical solutions have been derived. The expression relating conversion, c, and the enantiomeric excess of the starting material, $\mathrm{ee}_{\mathrm{sm}}$, to k_{rel} is illustrated in eq 2 for the case of first-order kinetics ($m = 1$) for a racemic mixture of substrates.

$$R \xrightarrow{k_R} P_R \qquad S \xrightarrow{k_S} P_S \qquad \frac{dR/dt}{dS/dt} = \frac{dR}{dS} = k_{rel}\frac{[R]^m}{[S]^m} \tag{1}$$

$$k_{\mathrm{rel}}^{\text{1st order}} = \frac{\ln[(1-c)(1-\mathrm{ee}_{\mathrm{sm}})]}{\ln[(1-c)(1+\mathrm{ee}_{\mathrm{sm}})]} \tag{2}$$

Recently, the concept of kinetic resolution has been extended to the case where enantioimpure catalysts are used. Ismagilov[2] and Kagan and co-workers[3] both noted that the observed selectivity factor will be much lower than the intrinsic selectivity factor derived for the enantiopure case. Kagan[3] and Johnson and Singleton[4] each extended this discussion to cases where the enantioimpure catalyst exhibits nonlinear effects due to formation of dimeric or higher-order catalyst species,[5] and they noted that asymmetric amplifications are possible in these cases.

This paper describes unexpected behavior in kinetic resolutions using enantioimpure catalysts which may be predicted in cases where the catalytic reactions exhibit complex reaction rate laws. We show that the selectivity factor may change significantly with conversion of substrate because of the intrinsic "kinetic partitioning" of the catalyst between different intermediate species in the catalytic network.[6] Kinetic partitioning offers a mechanism for asymmetric amplification which may complement, and in some cases magnify, the nonlinear effects due to catalyst interactions described by Kagan's ML_n models in kinetic resolutions employing enantioimpure catalysts.[3,4]

In addition, it is demonstrated that the conversion dependence of the selectivity factor in reactions using enantioimpure catalysts may be used to extract information about rate and binding constants which may be extended to the enantiopure case. Therefore, such experiments may be a valuable mechanistic tool even in cases where classic nonlinear behavior is not expected.

The kinetics governing catalytic reactions are generally not described by simple power-law rate expressions, because they involve at least one substrate-binding step to a catalyst species which is then regenerated at the end of each catalytic turnover. When enantioimpure catalysts are employed in kinetic resolutions, the equations derived to describe the selectivity factor for simple first- and second-order kinetics may not always be valid, and a conversion-dependent selectivity factor may be obtained. This apparently anomalous behavior during kinetic resolution is solely a consequence of the intrinsic kinetic rate

---

(1) (a) Kagan, H. B.; Fiaud, J. C. In *Topics in Stereochemistry*; Eliel, E. L., Wilen, S. H., Eds.; John Wiley & Sons: New York, 1988; Vol. 18, pp 249−330. (b) Sih, C. J.; Wu., S. H. In *Topics in Stereochemistry*; Eliel, E. L., Wilen, S. H., Eds.; John Wiley & Sons: New York, 1988; Vol. 19, pp 63−125.

(2) Ismagilov, R. F. *J. Org. Chem.* **1998**, *63*, 3772−3774.

(3) Luukas, T. O.; Girard, C.; Fenwick, D. R.; Kagan, H. B. *J. Am. Chem. Soc.* **1999**, *121*, 9299−9306.

(4) Johnson, D. W.; Singleton, D. A. *J. Am. Chem. Soc.* **1999**, *121*, 9307−9312.

(5) (a) Girard, C.; Kagan, H. B. *Angew. Chem., Int. Ed.* **1998**, *37*, 2922. (b) Puchot, C.; Samuel, O.; Duñach, E.; Zhao, S.; Agami, C.; Kagan, H. B. *J. Am. Chem. Soc.* **1986**, *108*, 2353−2357. (c) Guillaneux, D.; Zhao, S. H.; Samuel, O.; Rainford, D.; Kagan, H. B. *J. Am. Chem. Soc.* **1994**, *116*, 9430−9439.

(6) Indeed, the possibility that the selectivity factor in kinetic resolution might vary with conversion in cases of complex kinetics was raised by Sih (ref 1b, p 67).

10.1021/ja002562o CCC: $20.00

Scheme 1. Reaction Mechanism for the Proposed Catalytic Cycle for Kinetic Resolution[a]

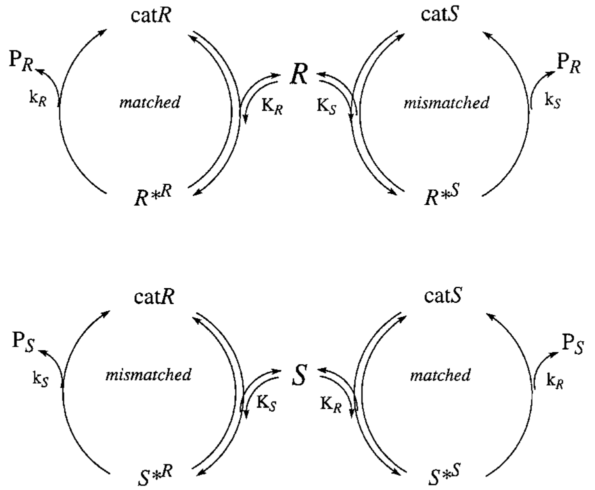

[a] Left half of the scheme shows the reactions of the *R* and *S* substrates employing enantiopure cat*R*; when an enantioimpure mixture of noninteracting catalysts is used, the right half of the scheme describing reactions employing cat*S* must also be considered.

law governing each reaction independently. Therefore observation of such behavior and its interpretation in terms of nonlinear models involving the formation of dimeric homochiral and heterochiral species could lead to erroneous mechanistic hypotheses. Conversely, monitoring catalytic behavior due to this kinetic partitioning may reveal significant detail about the reaction rate laws independently governing the parallel reactions in the kinetic resolution. Theoretical derivation of expressions describing kinetic resolutions in such cases are combined with reaction simulations to illustrate these points. Literature examples of experimental studies of kinetic resolution using enantioimpure catalysts are also discussed in the context of kinetic partitioning.

Kinetic Model: Enantiopure Catalysts

Catalytic reactions strictly do not obey simple elementary reaction rate expressions. However, the k_{rel} in a catalytic kinetic resolution using an enantiopure catalyst may in most cases be described by simple first- or second-order dependence on substrate concentrations, even though the kinetic rate law is more complex and the observed reaction order in such cases may even change over the course of the reaction. This may be shown by consideration of the reaction network shown in the left half of Scheme 1, which describes a kinetic resolution using catalysts which follow the simplest form of Michaelis−Menten kinetics. In this model, preequilibrium binding of the *R* and *S* substrates to an enantiopure catalyst, cat*R*, is followed by an irreversible product formation step. We assume that *R* is the faster-reacting substrate and we call this the *matched* reaction. The rate expressions for the *matched* and *mismatched* reactions, the consumption of [*R*] and [*S*], respectively, may be written as eqs 3 and 4:

$$-\frac{\mathrm{d}[R]}{\mathrm{d}t} = k_R[R{*}^R] = k_R K_R[R][\mathrm{cat}R] = \frac{k_R K_R[R][\mathrm{cat}R]_{\mathrm{total}}}{(1 + K_R[R] + K_S[S])} \tag{3}$$

$$-\frac{\mathrm{d}[S]}{\mathrm{d}t} = k_S[S{*}^R] = k_S K_S[S][\mathrm{cat}R] = \frac{k_S K_S[S][\mathrm{cat}R]_{\mathrm{total}}}{(1 + K_R[R] + K_S[S])} \tag{4}$$

The complexity in these rate expressions arises due to the denominator and deserves some comment because of its implications for reactions employing enantioimpure catalysts, to be discussed in the next section. Equations 3 and 4 share a common denominator which is comprised of several terms with dependences on the concentrations of both substrates. These terms represent the different ways in which the single catalyst precursor, $[\mathrm{cat}R]_{\mathrm{total}}$, partitions itself as intermediates species within the two catalytic cycles. Entry into the reaction cycle is through cat*R* for both the *R* and *S* reactions; cat*R* then partitions into [*R**] in the *R*-network and [*S**] in the *S*-network. Thus, the total catalyst concentration at any given time is given by eq 5, in which the preequilibrium assumption was invoked to solve for the intermediate species [*R**] and [*S**]. When we solve for [cat*R*] in terms of $[\mathrm{cat}R]_{\mathrm{total}}$, we obtain eq 6. The denominator is termed the "cat*R* denominator" to distinguish it from the case of enantioimpure catalysts to be discussed in the following sections.

$$[\mathrm{cat}R]_{\mathrm{total}} = [\mathrm{cat}R] + [R{*}^R] + [S{*}^R] = [\mathrm{cat}R](1 + K_R[R] + K_S[S]) \tag{5}$$

$$[\mathrm{cat}R] = \frac{[\mathrm{cat}R]_{\mathrm{total}}}{(1 + K_R[R] + K_S[S])} = \frac{[\mathrm{cat}R]_{\mathrm{total}}}{(\mathrm{cat}R\ \mathrm{denominator})} \tag{6}$$

These equations show that in any given reacting system obeying the mechanism in the left side of Scheme 1, where enantiopure catalyst $\mathrm{cat}R_{\mathrm{total}}$ is added to the reaction mixture, the *R* and *S* reaction cycles share the same pool of catalyst species. Hence, the denominator in the rate expressions describing the consumption of each substrate will be identical. When we take the ratio of *R* and *S* rates, these denominators will then cancel, as will the total catalyst concentration $[\mathrm{cat}R]_{\mathrm{total}}$, and in this case we are left with an expression reminiscent of a conventional first-order kinetic resolution (eq 7). It is interesting to note that for this simple example of preequilibrium kinetics, the selectivity factor k_{rel} describes the Curtin-Hammett limit[7] in which selectivity is dictated by both the stability (manifested by K_R and K_S) *and* the reactivity (manifested by k_R and k_S) of the intermediate species in each pathway.

$$\frac{\mathrm{d}[R]}{\mathrm{d}[S]} = \frac{k_R K_R[R]}{k_S K_S[S]} = k_{\mathrm{rel}}\frac{[R]}{[S]} \tag{7}$$

Thus, even for complex catalytic cycles, the expression for the selectivity factor in a kinetic resolution simplifies in most cases to that derived for simple first-order kinetics in substrate concentration. An important implication of this result is that the selectivity factor should be independent of substrate conversion for kinetic resolutions employing enantiopure catalysts.

Kinetic Model: Enantioimpure Catalysts

Noninteracting Catalysts (Linear Case). When a kinetic resolution is carried out using enantioimpure catalysts which do *not* interact with one another, the reaction network must be expanded to include both the right and left sides of Scheme 1. In this case four separate reaction cycles must be considered in which the rate and equilibrium constants are related in a simple manner. The cycles for the two *matched* interactions between catalyst and substrate shown on the upper left and lower right

---

[7] In the Curtin-Hammett limit, the substrate binding−dissociation equilibrium is fast and is therefore unperturbed by the subsequent product-forming step. For a comprehensive review, see: Seeman, J. I. *Chem. Rev.* **1983**, *83*, 83−134.

of Scheme 1 (cat$R + R$ and cat$S + S$) will be described by one set of rate and equilibrium constants (k_R and K_R), while the two *mismatched* cycles in the upper right and lower left of Scheme 1 (cat$R + S$ and cat$S + R$) will be described by a second set (k_S and K_S). Whereas the reaction rate expressions for consumption of R and S had a shared denominator when only $[\mathrm{cat}R]_{\mathrm{otal}}$ was present, the two cycles shown on the right side of Scheme 1 will give rate expressions with a different denominator describing the partitioning of $[\mathrm{cat}S]_{\mathrm{total}}$ in the cycle (eqs 8 and 9).

$$[\mathrm{cat}S]_{\mathrm{total}} = [\mathrm{cat}S] + [R^{*S}] + [S^{*S}] = [\mathrm{cat}S](1 + K_S[R] + K_R[S]) \quad (8)$$

$$[\mathrm{cat}S] = \frac{[\mathrm{cat}S]_{\mathrm{total}}}{(1 + K_S[R] + K_R[S])} = \frac{[\mathrm{cat}S]_{\mathrm{total}}}{(\mathrm{cat}S\ \mathrm{denominator})} \quad (9)$$

Now the overall rate of R consumption contains two terms representing the cycles in the upper half of Scheme 1, one matched and one mismatched reaction. The rate of S consumption similarly contains two terms corresponding to the lower half of Scheme 1 (eqs 10 and 11).

$$-\frac{\mathrm{d}[R]}{\mathrm{d}t} = k_RK_R[R][\mathrm{cat}R] + k_SK_S[R][\mathrm{cat}S] = \left[\frac{k_RK_R[\mathrm{cat}R]_{\mathrm{total}}}{(1 + K_R[R] + K_S[S])} + \frac{k_SK_S[\mathrm{cat}S]_{\mathrm{total}}}{(1 + K_S[R] + K_R[S])}\right][R] \quad (10)$$

$$-\frac{d[S]}{dt} = k_SK_S[S][\mathrm{cat}R] + k_RK_R[S][\mathrm{cat}S] = \left[\frac{k_SK_S[\mathrm{cat}R]_{\mathrm{total}}}{(1 + K_R[R] + K_S[S])} + \frac{k_RK_R[\mathrm{cat}S]_{\mathrm{total}}}{(1 + K_S[R] + K_R[S])}\right][S] \quad (11)$$

It is easy to see that when we divide the two rates the denominators will no longer cancel.

Because these two denominators may exhibit different concentration dependences, the selectivity factor in kinetic resolution using enantioimpure catalysts may vary with conversion (eq 12).

$$k_{\mathrm{rel}} = \left[\frac{k_RK_R[\mathrm{cat}R] + k_SK_S[\mathrm{cat}S]}{k_SK_S[\mathrm{cat}R] + k_RK_R[\mathrm{cat}S]}\right] \quad (12a)$$

$$= \frac{\dfrac{k_RK_R}{(\mathrm{cat}R\ \mathrm{denominator})}[\mathrm{cat}R]_{\mathrm{total}} + \dfrac{k_SK_S}{(\mathrm{cat}S\ \mathrm{denominator})}[\mathrm{cat}S]_{\mathrm{total}}}{\dfrac{k_SK_S}{(\mathrm{cat}R\ \mathrm{denominator})}[\mathrm{cat}R]_{\mathrm{total}} + \dfrac{k_RK_R}{(\mathrm{cat}S\ \mathrm{denominator})}[\mathrm{cat}S]_{\mathrm{total}}} \quad (12b)$$

Under some conditions, a constant k_{rel} will be observed for systems following these kinetics. For example, if the binding constants for the matched and mismatched substrates are equal, the denominators will be equal and will again cancel in the equation describing the ratio of rates. If K_R and K_S are both very low, and if very low substrate concentrations are employed, the concentration terms in each denominator will be small compared to one, and the rate expression will be dictated by the numerator alone. In either of these cases, the *s*-factor will be a function only of the binding and rate constants and the total concentrations of the two catalysts, all of which are constants. The selectivity factor is then given by eq 13. This is the case described in both Kagan's[3] and Singleton's[4] recent treatments.

$$k_{\mathrm{rel}} = \frac{k_RK_R[\mathrm{cat}R]_{\mathrm{total}} + k_SK_S[\mathrm{cat}S]_{\mathrm{total}}}{k_SK_S[\mathrm{cat}R]_{\mathrm{total}} + k_RK_R[\mathrm{cat}S]_{\mathrm{total}}} \quad (13)$$

The resemblance between eqs 13 and 12 is interesting to note. An apparent nonlinear effect will observed if we expect the concentrations [cat$R$] and $[\mathrm{cat}R]_{\mathrm{total}}$ (also [cat$S$] and $[\mathrm{cat}S]_{\mathrm{total}}$) to be linearly related to one another as conversion increases. If we calculate the catalyst enantiomeric excess based on [cat$R$] and [cat$S$] rather than the total catalyst concentrations, we can see that this ee changes over the course of the reaction (eq 14).

$$ee_{cat} = \frac{[\mathrm{cat}R] - [\mathrm{cat}S]}{[\mathrm{cat}R] + [\mathrm{cat}S]} = \frac{\dfrac{[\mathrm{cat}R]_{\mathrm{total}}}{(1 + K_R[R] + K_S[S])} - \dfrac{[\mathrm{cat}S]_{\mathrm{total}}}{(1 + K_S[R] + K_R[S])}}{\dfrac{[\mathrm{cat}R]_{\mathrm{total}}}{(1 + K_R[R] + K_S[S])} + \dfrac{[\mathrm{cat}S]_{\mathrm{total}}}{(1 + K_S[R] + K_R[S])}} \quad (14)$$

This effective $\mathrm{ee}_{\mathrm{cat}}$ is a result of what might be termed a "kinetic partitioning" of $[\mathrm{cat}R]_{\mathrm{total}}$ and $[\mathrm{cat}S]_{\mathrm{total}}$ into the various intermediate species within the catalytic cycle which changes over the course of the reaction.

In many kinetic resolution processes, discrimination between the rates of consumption of the two enantiomeric substrates comes about because of a significant difference in their binding strengths. In such cases it may be expected that the *s*-factor and the effective $\mathrm{ee}_{\mathrm{cat}}$ will vary significantly with conversion in kinetic resolutions using enantioimpure catalysts. This intrinsic kinetic phenomenon will manifest itself as a nonlinear effect in catalyst enantiopurity, even in the absence of interaction between catalyst species, with important implications for practical efficiency as will be shown later in this paper.

Interacting Catalysts (Nonlinear Case). It is possible that the "kinetic partitioning" described in the previous section may occur in catalytic reactions which also exhibit a classic nonlinear effect involving the interaction between catalyst species to form dimeric or higher-order species. In this case the observed anomalous behavior will be due to the combination of the effects of this interaction and the intrinsic kinetic effect. The model most commonly used to describe interactions between catalysts is Kagan's ML_2 model[5] where three separate dimeric catalysts, [catRR], [catSS], and [catRS], are present in the system. The catalytic cycle for such a system undergoing kinetic resolution is shown in Scheme 2 for the case of Michaelis−Menten kinetics discussed in the previous section. The catalytic cycles for the two homochiral species will be analogous to those for [cat$R$] and [cat$S$] in the case shown in Scheme 1. The third catalyst, the *meso* species [catRS], will bind each enantiomer equally with its own binding constant K_{RS}, and it will react with each enantiomer equally with its own rate constant k_{RS}. This means that in any expression describing a kinetic resolution for this case, there will now be three different denominators to consider (eqs 15 and 16).

$$[\mathrm{cat}RR] = \frac{[\mathrm{cat}RR]_{\mathrm{total}}}{(1 + K_{RR}[R] + K_{SS}[S])} = \frac{[\mathrm{cat}RR]_{\mathrm{total}}}{(\mathrm{cat}RR\ \mathrm{denominator})}$$

$$[\mathrm{cat}SS] = \frac{[\mathrm{cat}SS]_{\mathrm{total}}}{(1 + K_{SS}[R] + K_{RR}[S])} = \frac{[\mathrm{cat}SS]_{\mathrm{total}}}{(\mathrm{cat}SS\ \mathrm{denominator})}$$

$$[\mathrm{cat}RS] = \frac{[\mathrm{cat}RS]_{\mathrm{total}}}{(1 + K_{RS}([R] + [S]))} = \frac{[\mathrm{cat}SS]_{\mathrm{total}}}{(\mathrm{cat}RS\ \mathrm{denominator})} \quad (15)$$

Scheme 2. Reaction Mechanism for the Proposed Catalytic Cycle for Kinetic Resolution Shown in Scheme 1, Extended to the Case Where Two Homochiral (cat*RR* and cat*SS*) and One Heterochiral (cat*RS*) Catalyst Species Participate in the Reaction[a]

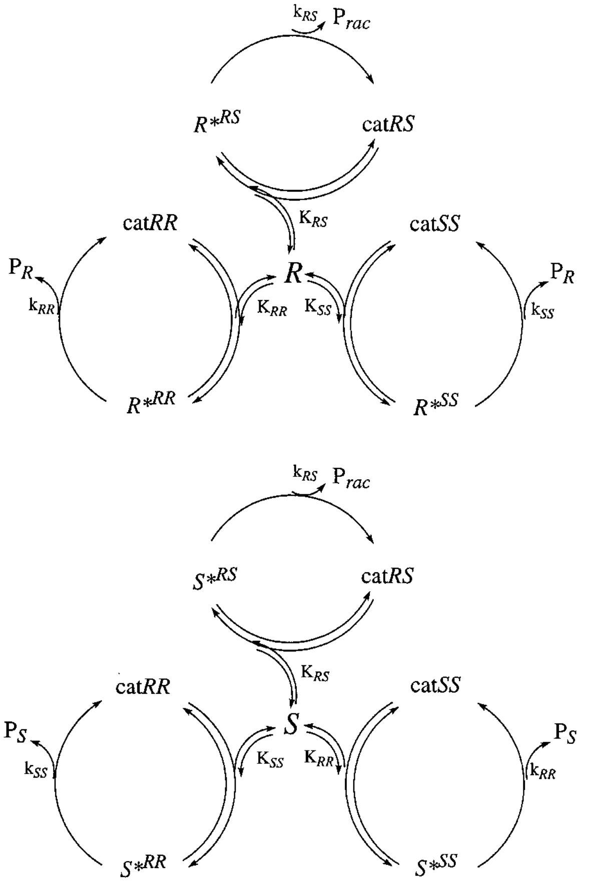

[a] Reaction of each substrate involves three separate catalytic cycles. The distribution of catalysts is determined by applying a model for nonlinear effects such as the ML$_2$ model, $K = [\text{cat}RS]/([\text{cat}RR][\text{cat}SS])$.

$$k_{\text{rel}} = \frac{\left[\dfrac{k_{RR}K_{RR}[\text{cat}RR]_{\text{total}}}{(\text{cat}RR\ \text{denominator})}\right]}{\left[\dfrac{k_{SS}K_{SS}[\text{cat}RR]_{\text{total}}}{(\text{cat}RR\ \text{denominator})}\right]} + \frac{\left[\dfrac{k_{SS}K_{SS}[\text{cat}SS]_{\text{total}}}{(\text{cat}SS\ \text{denominator})}\right]}{\left[\dfrac{k_{RR}K_{RR}[\text{cat}SS]_{\text{total}}}{(\text{cat}SS\ \text{denominator})}\right]} + \frac{\left[\dfrac{k_{RS}K_{RS}[\text{cat}RS]_{\text{total}}}{(\text{cat}RS\ \text{denominator})}\right]}{\left[\dfrac{k_{RS}K_{RS}[\text{cat}RS]_{\text{total}}}{(\text{cat}RS\ \text{denominator})}\right]} \tag{16}$$

All three denominators are functions of the *R* and *S* concentrations, and again the selectivity factor may change with conversion (unless K_{RR}, K_{SS}, and K_{RS} are equal or small compared to one). An observed nonlinear effect in catalyst enantiopurity in kinetic resolution may thus be the consequence of two separate phenomena, both of which cause "nonlinear partitioning" of the total catalyst concentrations: "classic" nonlinear partitioning of the *R* and *S* ligands into homochiral $[\text{cat}RR]_{\text{total}}$, $[\text{cat}SS]_{\text{total}}$, and heterochiral $[\text{cat}RS]_{\text{total}}$, and "kinetic" partitioning of $[\text{cat}RR]_{\text{total}}$, $[\text{cat}SS]_{\text{total}}$, and $[\text{cat}RS]_{\text{total}}$ into the intermediate species found within each catalytic cycle. The first is a function of the nature of the catalyst species themselves and is independent of the extent of reaction, while the second is an intrinsic property of the catalytic reaction cycle and is a function of conversion.

Results

Reaction simulations based on the Michaelis–Menten model presented in Scheme 1 were carried out to explore the effects of the intrinsic "kinetic partitioning" discussed above. The extension of this model to the case where the classic nonlinear effect described by the ML$_2$ model of catalyst interaction is combined with this effect (Scheme 2) is also illustrated with reaction simulations. Several literature examples of nonlinear effects in kinetic resolution are then discussed in terms of these concepts. Finally, practical implications of the use of enantioimpure catalysts for mechanistic analysis and catalyst design in kinetic resolutions are highlighted.

Noninteracting Catalysts (Linear Case). Kinetic resolutions were simulated for racemic mixtures of substrates *R* and *S* using enantioimpure mixtures of catalysts cat*R* and cat*S*. It is assumed that the system follows the complete reaction network shown in Scheme 1 and that the reactions of the two substrates obey the rate laws given in eqs 10 and 11. We assume that matched interactions in Scheme 2 give faster reactions and that cat*R* is in excess. Hence the enantiomeric excess of the remaining starting material at any time during the kinetic resolution represents the excess of *S* compared to *R* (eq 17).

$$\text{ee}_{\text{sm}} = \frac{[S] - [R]}{[S] + [R]} \tag{17}$$

The course of the kinetic resolution was simulated for reactions employing catalysts at various levels of enantiopurity with selectivity factors k_{rel} for an enantiopure catalyst cat*R* between 5 and 100 ($k_{\text{rel}} = k_R K_R / k_S K_S$). Kinetic resolutions were simulated for two opposite cases of substrate binding, one where the matched interactions in Scheme 1 exhibit stronger binding compared to the mismatched case ($K_R = 10K_S$) and one for the converse ($K_S = 10K_R$). From the work of Ismagilov[2] and Kagan and co-workers,[3] the expected linear value at any ee_{cat} for a first-order kinetic resolution may be calculated. For example, when $k_{\text{rel}} = 20$ employs an enantiopure catalyst, the k_{rel} for the same resolution using enantioimpure catalysts at $\text{ee}_{\text{cat}} = 0.7$, 0.5, and 0.25 will decrease to 4.5, 2.7, and 1.6, respectively (assuming no nonlinear effect due to catalyst interaction). In our simulation using the Michaelis–Menten kinetic model, the values predicted for the linear case represent the selectivity factor at the outset of the reaction (conversion = 0). For ease of combining data at different values of ee_{cat} into one plot, selectivity factors are normalized to those calculated at the outset of each reaction. Therefore, deviation from $s_{\text{norm}} = 1$ indicates the extent of deviation from the behavior expected for a first-order kinetic resolution.

Figure 1 demonstrates how this selectivity factor changes over the course of the kinetic resolution when catalysts of differing enantiopurity are employed. Figure 1a shows that when the "matched" interaction has stronger binding, the selectivity factor can increase significantly with conversion. For example, for a catalyst enantiopurity of 50%, the selectivity factor observed at 80% conversion is nearly 4 times higher than that observed at the outset of the reaction. By contrast, stronger binding of the "mismatched" interaction yields a trend of decreasing k_{rel} with conversion of substrate (Figure 1b).

As discussed above, this changing selectivity factor comes about due to a change in the partitioning of the catalytic species in the network over the course of the reaction. This is illustrated in Figure 2 for the kinetic resolutions shown in Figure 1. Figure 2a shows how the effective catalyst ee (based on eq 14) increases with conversion for a stronger matched substrate/catalyst

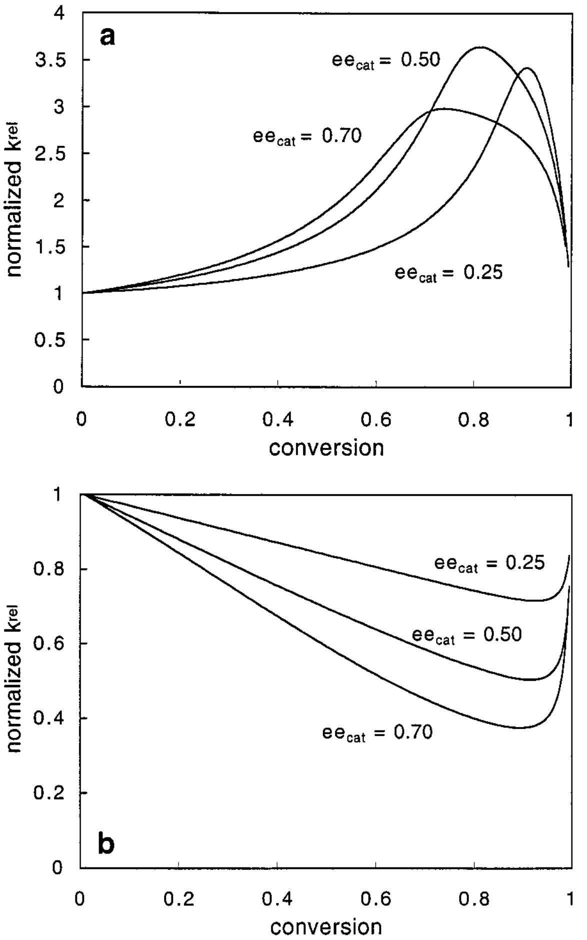

Figure 1. Normalized selectivity factor k_{rel} as a function of substrate conversion for kinetic resolutions of racemic substrates using enantioimpure catalysts. Reactions are simulated according to the mechanism in Scheme 1 for the case where the enantiopure catalyst gives $k_{rel} = k_RK_R/k_SK_S = 20$. Selectivity factors are normalized to the value found at conversion = 0. (a) Stronger binding for "matched" substrate-catalyst interaction: $K_R = 10K_S$. (b) Stronger binding for "mismatched" substrate-catalyst interaction: $K_S = 10K_R$.

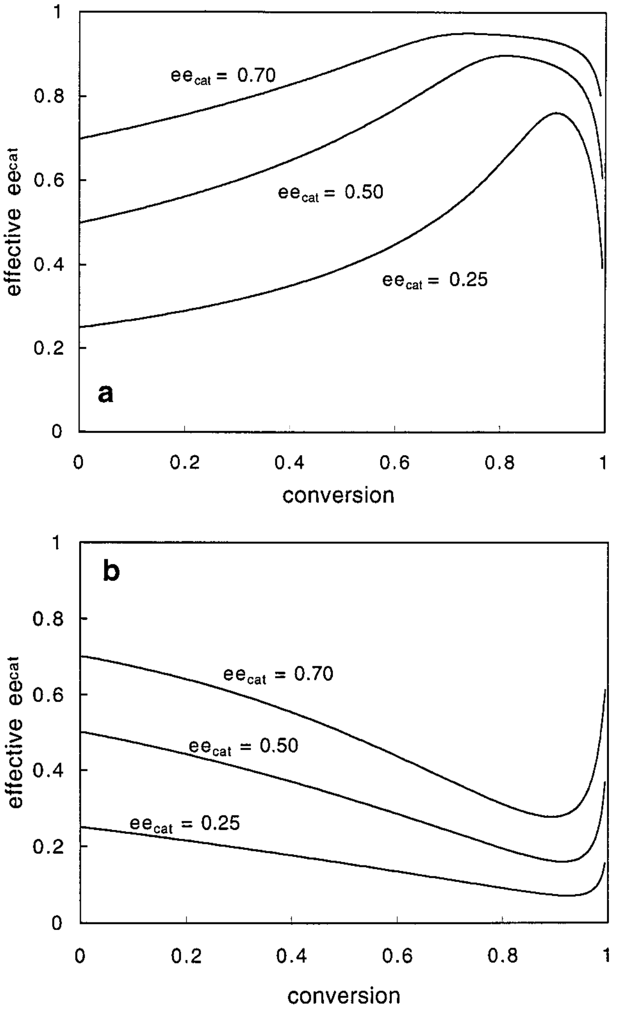

Figure 2. Apparent catalyst enantiomeric excess as a function of conversion for the kinetic resolution described in Figure 1, calculated according to eq 14. (a) Stronger binding for "matched" substrate-catalyst interaction: $K_R = 10K_S$. (b) Stronger binding for "mismatched" substrate-catalyst interaction: $K_S = 10K_R$.

binding, while Figure 2b shows that the converse occurs with stronger binding in the mismatched case.

Complex kinetic expressions may also influence how the ee of the starting material increases with substrate conversion in kinetic resolutions with enantioimpure catalysts. This is illustrated in Figure 3 from the kinetic resolutions described in Figures 1 and 2 for the case of $ee_{cat} = 0.25$ (Figure 3a) and $ee_{cat} = 0.7$ (Figure 3b). The ee of the starting material, ee_{sm}, is shown in each plot as a function of conversion for the two cases of relative substrate binding constants, and these are compared to the case of a conventional first-order kinetic resolution where the selectivity factor remains unchanged with conversion (given by eq 2). Asymmetric amplification is observed in the case where the matched substrate/catalyst binding is stronger, while the case of stronger mismatched binding gives a lower ee_{sm}-conversion profile than is predicted from the conventional first-order equation. The asymmetric amplification in the matched case is most significant at lower ee_{cat} values: at 90% conversion, the ee of the starting material reaches 94%, where an ee of 50% is predicted at this conversion level for the standard first-order case.

It might be suggested that the complication of a changing selectivity factor be avoided by using initial rate measurements to calculate k_{rel}. Indeed, Figure 1 shows that both positive and negative effects of kinetic partitioning show small overall deviation from standard first-order kinetics (less than 20%) at conversions less than 20%. However, initial rate measurements could provide misleading mechanistic and practical information for a system exhibiting this type of behavior. Predictions of the efficiency of kinetic resolution would be incorrect in cases where the reaction is to be carried out to higher conversions with the goal of enantiopurification of the substrate. Additionally, comparison between initial rate and higher conversion selectivity factors may aid in distinguishing between a kinetic partitioning effect and a classic nonlinear effect described by the ML_n models (see next section).

Figure 4 shows that the deviation from conventional first-order behavior becomes starker as the selectivity factor increases. For a catalyst at $ee_{cat} = 0.5$, an initial selectivity factor of 5 increases by a modest 50% at high conversion, while an initial selectivity factor of 100 can be seen to increase almost 6-fold at high conversion. In each case a steep rise in selectivity factor comes about at conversions where the fast-reacting substrate concentration approaches zero. This is illustrated in Figure 5, which plots fractional concentrations of [*R*] and [*S*] as a function of conversion for the case of $k_{rel} = 100$ and $ee_{cat} = 0.5$ from Figure 5. The predicted consumption of [*R*] and [*S*] as a function of conversion for the case of standard first-order kinetics is plotted as the dashed lines in Figure 5 for comparison.

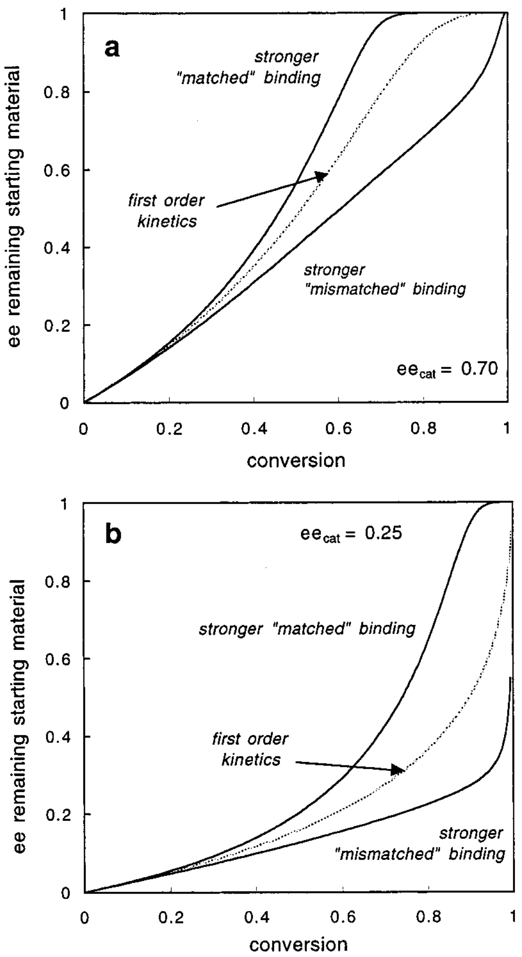

Figure 3. Enantiomeric excess of the remaining starting material as a function of conversion for the kinetic resolution described in Figure 1. The two opposite cases of substrate binding ($K_R = 10K_S$ and $K_S = 10K_R$) are compared to the case of conventional first-order kinetics. (a) $ee_{cat} = 0.70$. (b) $ee_{cat} = 0.25$.

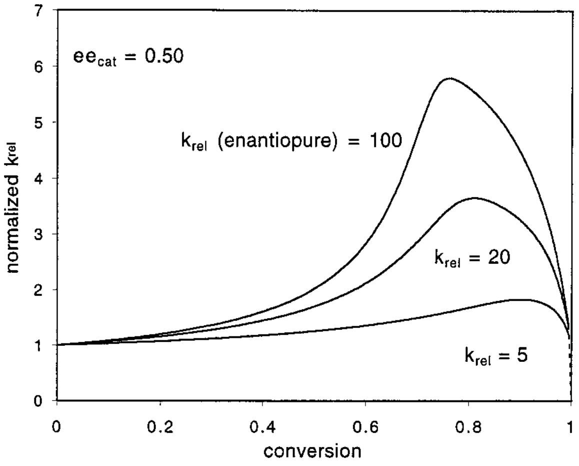

Figure 4. Normalized selectivity factor k_{rel} as a function of substrate conversion for kinetic resolutions of racemic substrates as shown in Scheme 1, using $ee_{cat} = 0.50$. Reactions are simulated for selectivity factors of $k_{rel} = 100$, 20, and 5 in the enantiopure case.

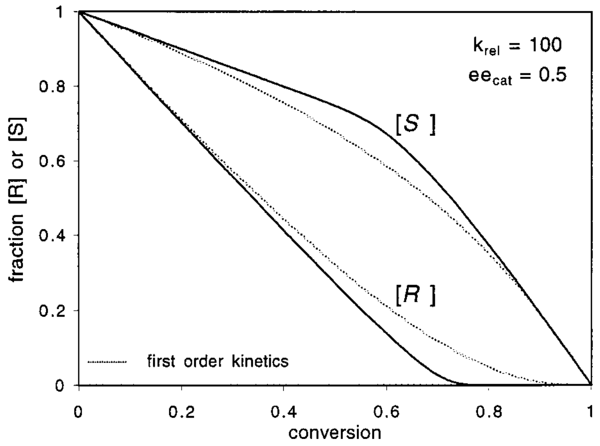

Figure 5. Fraction of [R] and [S] remaining as a function of conversion for a kinetic resolution simulated according to the mechanism in Scheme 1 using $ee_{cat} = 0.50$ and $k_{rel} = 100$ (enantiopure case). The dashed lines show the comparison to first-order kinetics.

Thus, it may be seen that two factors contribute to the asymmetric amplification observed as a function of conversion. The stronger matched case binding means that most of [cat$R$], which is in excess, will be occupied with R-binding until [R] is mostly consumed. Therefore, a faster rate of R-consumption compared to first-order kinetics is observed. In addition, the rate of S-consumption is inhibited compared to first-order kinetics because S cannot compete effectively for cat$R$ binding sites until the R-substrate concentration becomes small.

It is important to emphasize that the asymmetric amplifications and depletions described here do *not* arise because of formation of homochiral and heterochiral dimer species as described in the ML_2 model proposed by Kagan[5] to rationalize nonlinear effects in asymmetric synthesis. The nonlinearity in these cases has its origin solely in the intrinsic kinetic rate expressions from the independent reactions of the enantiomeric catalyst species in the reaction mixture, according to the four concurrent catalytic cycles shown in Scheme 1. Thus, the intrinsic kinetics of the reaction scheme itself can aid or hinder the efficiency of kinetic resolution when enantioimpure catalysts are employed.

Interacting Catalysts (Nonlinear Case). The case of kinetic resolution using enantioimpure catalysts which interact in solution offers the possibility of nonlinear behavior arising from two separate sources, as discussed in a previous section and shown in Scheme 2. The possible effects offered by the combination of the two types of nonlinearity are myriad, with additional variables including the rate and binding constants for the *meso* species (catRS) as well as the relative distribution of *meso* and enantiopure (catRR and catSS) species. For the purposes of this illustration, we simulate a kinetic resolution in which the catalyst distribution is statistical (the relative catalyst concentrations at any catalyst enantiopurity are given by $K = 4 = [\mathrm{cat}RS]^2/([\mathrm{cat}RR][\mathrm{cat}SS])$) and the rate of reaction for the pathway involving catRS is slow ($k_{RS} = 0.05k_{RR}$), and a selectivity factor of $k_{rel} = 20$ is observed for the enantiopure catalyst. In the absence of any kinetic partitioning effect, these conditions describe a case of asymmetric amplification in kinetic resolution. We shall consider the case where the binding constants for both the matched substrate−catalyst species and the *meso* species are high compared to the mismatched case ($K_{RR} = K_{RS} = 10K_{SS}$).

Figure 6 plots the ee of the starting material as a function of conversion for $ee_{cat} = 0.5$. Three different cases are compared. Simple first-order “linear” kinetics in the absence of any catalyst interaction ([catRS] = 0) is given in Figure 6a. In Figure 6b, the reaction again follows simple first-order kinetics, but in this case the catalyst distribution is nonlinear and follows the ML_2 model with parameters described above. In Figure 6c, this nonlinear ML_2 model is combined with the effects of kinetic partitioning due to a complex kinetic rate law. We can see that

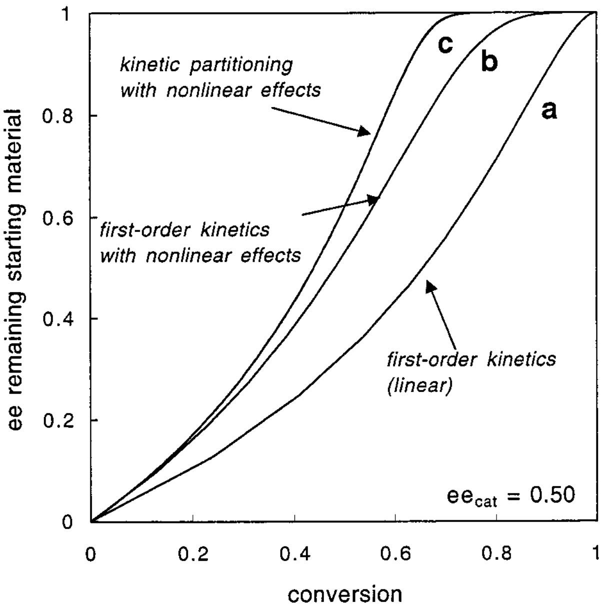

Figure 6. Enantiomeric excess of the remaining starting material as a function of conversion for kinetic resolution as shown in Scheme 2, for $ee_{cat} = 0.50$. The selectivity factor for the enantiopure case is $k_{rel} = 20$. (a) First-order kinetics in the absence of a nonlinear effect ([cat*RS*] = 0). (b) First-order kinetics incorporating a nonlinear effect according to the ML_2 model, with three catalytic cycles based on two homochiral and one heterochiral catalyst with the distribution of catalyst species given by $K = 4$ and the relative reactivity of the heterochiral catalyst cat*RS* given by k_{RS} = = $0.05k_{RR}$. (c) Reaction network following the catalytic rate law given in eq 16 *and* incorporating a nonlinear effect, with the initial distribution and relative reactivity of catalyst species as in (b). Strong binding of the fast-reacting substrate to the homochiral catalyst cat*RR* and to the *meso* catalyst cat*RS* is assumed ($K_{RR} = K_{RS} = 10K_{SS}$).

in this case the asymmetric amplification observed due to the ML_2 model is further enhanced when combined with the effect arising from kinetic partitioning. Kagan has noted that the superposition of an asymmetric amplification in a kinetic resolution leads to a double amplification of chirality, since the resolution is itself an amplification by means of partial conversion of a racemic substrate;[3] this example shows how the intrinsic reaction kinetics can lead to a *trebling* effect by overlaying a third amplification mechanism, that of kinetic partitioning. Thus, the superposition of the two phenomena, kinetic partitioning and catalyst aggregation, can lead to increased efficiency in kinetic resolution.[8]

Experimental Examples of Nonlinear Behavior in Kinetic Resolution

Kinetic Resolution of Sulfoxides. In one early experimental report of kinetic resolution using enantioimpure catalysts, Uemura and co-workers[9] observed an asymmetric amplification in the resolution of racemic sulfoxides catalyzed by chiral Ti−binaphthol complexes (eq 18).

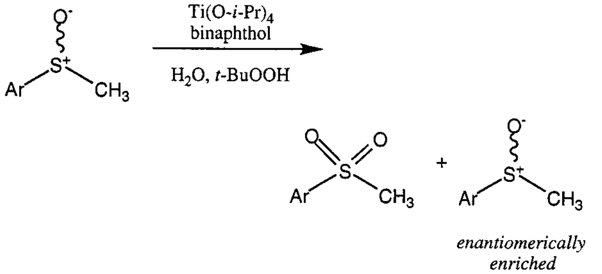

(18)

The nonlinear effect was found to be quite significant at higher conversions of the substrate. Figure 7 shows a plot of ee of remaining starting material versus ee_{cat} for data obtained at high conversion, taken from ref 6. The dashed line shows the expected trend for simple first-order kinetics in the absence of a nonlinear effect. When we consider these data in terms of our kinetic model, we find that the experimental data are well described by the kinetic partitioning effect under conditions where an asymmetric amplification occurs, as shown by the solid line in Figure 7. This result was obtained *without* invoking nonlinear effects due to catalyst interaction. Thus, kinetic partitioning might be considered to be a contributing factor to the asymmetric amplification in this case. However, it is important to note that mechanistic information concerning the reaction described in ref 6 is scarce. Indeed, the selectivity factor was observed to vary significantly with conversion even in the case of enantiopure catalysts. Thus, the reaction is most certainly more complex than may be simply described either by an ML_2 model for catalyst interaction or by the kinetic partitioning discussed here.

Hydrolytic Kinetic Resolution of Epoxides. In a recent example of kinetic resolution using enantioimpure catalysts, Johnson and Singleton[4] carried out Jacobsen's hydrolytic kinetic resolution[10] using (salen)Co catalysts of varying enantiopurity (eq 19). Jacobsen observed a second-order dependence on catalyst concentration in this reaction and in the related asymmetric ring-opening of *meso* epoxides using (salen)Cr complexes.[11] In that case, they also observed nonlinear effects in catalyst enantiopurity.

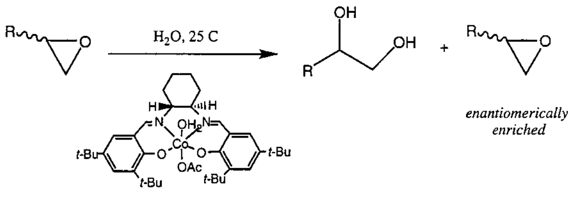

(19)

Johnson and Singleton observed an asymmetric amplification in this hydrolytic kinetic resolution carried out using enantioimpure catalysts.They introduced a term called a "differential kinetic enantiomeric enhancement", or DKEE (eq 20), in their development of equations analogous to Kagan's ML_2 model for application to nonlinear effects in kinetic resolutions. The DKEE provides a way to plot information about the selectivity factor as a function of catalyst enantiopurity so that it may be compared to the linear case, analogous to plots of product enantioselectivity versus ee_{cat} used in the ML_n models to describe nonlinear effects in asymmetric synthesis involving enantioimpure catalysts.

$$\mathrm{DKEE} = \frac{k_{rel} - 1}{k_{rel} + 1} = \mathrm{DKEE}_0 \cdot \mathrm{ee}_{cat} \cdot \frac{1 + \beta}{1 + g\beta}$$

$$\beta = \frac{[\mathrm{cat}RS]}{[\mathrm{cat}RR] + [\mathrm{cat}SS]}; \quad g = \frac{2k_{RS}}{k_{RR} + k_{SS}} \quad (20)$$

The ratio of rates of R- and S-consumption was given by eq 21.

$$\frac{d[R]}{d[S]} = \frac{k_{RR}[\mathrm{cat}RR] + k_{SS}[\mathrm{cat}SS] + k_{RS}[\mathrm{cat}RS]}{k_{SS}[\mathrm{cat}RR] + k_{RR}[\mathrm{cat}SS] + k_{RS}[\mathrm{cat}RS]} \cdot \frac{[R]}{[S]} = k_{rel} \cdot \frac{[R]}{[S]} \quad (21)$$

This equation implies that any "kinetic partitioning" is negligible, since the selectivity factor is treated as a constant. As we have shown, this treatment will not be able to account for changing concentrations of the various intermediate species within the catalytic cycle over the course of the reaction. More significantly, the complex kinetics of the catalytic cycle in the case of the Jacobsen HKR indicate that nonlinear

---

[8] Kinetic partitioning may also work in the opposite direction from that of a classic asymmetric amplification, in the case where binding of the slower-reacting substrate is stronger. In this case, if the two effects were superimposed in the same system, efficiency would be decreased.

[9] Komatsu, N.; Hashizume, M.; Sugita, T.; Uemura, S. *J. Org. Chem.* **1993**, *58*, 7624−7626.

[10] Tokunaga, M.; Larrow, J. F.; Kakiuchi, F.; Jacobsen, E. N. *Science* **1997**, *277*, 936.

[11] Konsler, R. G.; Karl, J.; Jacobsen, E. N. *J. Am. Chem. Soc.* **1998**, *120*, 10780.

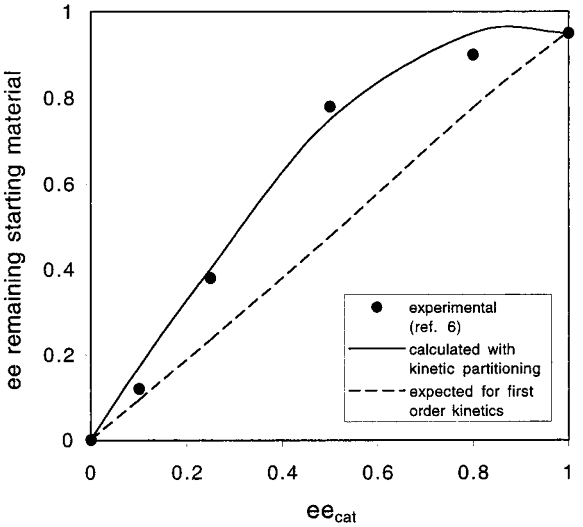

Figure 7. Enantiomeric excess of the starting material remaining at 70−75% conversion of substrate as a function of catalyst enantiopurity for the kinetic resolution of racemic sulfoxides according to eq 18. Filled circles represent experimental data points taken from ref 6. The dashed line gives the predicted relationship for first-order kinetics, which appears quasi-linear for systems exhibiting k_{rel}(enantiopure) < ~10. The solid line is derived from simulations of the reaction according to eqs 10−12, assuming two independent catalyst species with no interaction. The selectivity factor for the enantiopure catalyst $k_{rel} = 8$, and $K_R = 10K_S$.

Scheme 3. Reaction Pathways for Kinetic Resolution of Racemic Epoxides (Eq 18) Using Enantioimpure Catalysts According to a Binuclear Catalyst Mechanism[a]

$$\text{pathway }(1)\quad R\text{-}catR + N\text{-}catR \xrightarrow{k_1}$$

$$\text{pathway }(2)\quad R\text{-}catS + N\text{-}catR \xrightarrow{k_2}$$

$$\text{pathway }(3)\quad R\text{-}catR + N\text{-}catS \xrightarrow{k_3}$$

$$\text{pathway }(4)\quad R\text{-}catS + N\text{-}catS \xrightarrow{k_4}$$

$$\text{pathway }(5)\quad S\text{-}catR + N\text{-}catR \xrightarrow{k_5}$$

$$\text{pathway }(6)\quad S\text{-}catS + N\text{-}catR \xrightarrow{k_6}$$

$$\text{pathway }(7)\quad S\text{-}catR + N\text{-}catS \xrightarrow{k_7}$$

$$\text{pathway }(8)\quad S\text{-}catS + N\text{-}catS \xrightarrow{k_8}$$

[a] *R*, *S*, and *N* represent, respectively, the epoxide enantiomers and the nucleophile (H_2O), and are depicted as bound either to catalyst species cat*R* or cat*S*. The rate expressions for this mechanism will be of the form of eq 22 or eq 23.

effects in such a system are qualitatively different from the model proposed by Johnson and Singleton. The observation of second-order kinetics in catalyst concentration was rationalized by Jacobsen with the proposal of a bi-nuclear role for the catalyst: a nucleophile (*N*) bound to one catalyst species is delivered to an electrophile (*R* or *S*) bound to a second catalyst species. For the kinetic resolution of chiral substrates using enantioimpure catalysts, eight possible reaction pathways may be envisioned as shown in Scheme 3. Since each pathway involves two separate monomeric catalysts, all catalyst terms in the corresponding rate expressions will be squared.

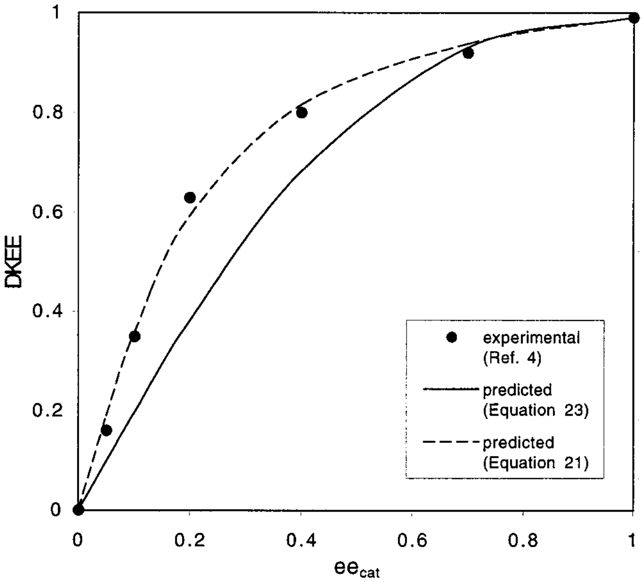

Figure 8. Differential kinetic enantiomeric excess as a function of catalyst enantiopurity for the hydrolytic kinetic resolution of 1-pentene oxide according to eq 18.

Scheme 3 has important implications for quantifying the role of kinetic partitioning in this reaction network. The denominators of the rate expressions which describe the cat*R*−cat*R* and cat*S*−cat*S* interactions (pathways 1, 4, 5, and 8) will each be raised to the second power. The denominator for the four potential "matched−mismatched" interactions (pathways 2, 3, 6, and 7) will be identical and will be described by multiplying the cat*R* and cat*S* denominators together. All of these denominators will contain concentration dependences for both substrates. We combine all rate and equilibrium constants into parameters k_1−k_8 for the reaction pathway outlined in Scheme 3. For symmetry reasons it may also be shown that $k_1 = k_8$ (designated k_R), $k_4 = k_5$ (designated k_S), and $k_2 + k_3 = k_6 + k_7$ (designated k_{RS}). If we give the cat*R* and cat*S* denominators the designations "cat*R*-denom" and "cat*S*-denom", respectively, the rate expression describing the kinetic resolution will take the form of eq 22. Quantitative determination of the form of the cat*R* and cat *S* denominators as well as the reaction order in *R* and *S* substrates in the numerator would require detailed experimental kinetic studies.

$$\frac{d[R]}{d[S]} = k_{rel}\cdot\frac{f[R]}{f[S]}$$

$$k_{rel} = \frac{\dfrac{k_R[\text{cat}R]^2_{total}}{(\text{cat}R\text{-denom})^2} + \dfrac{k_S[\text{cat}S]^2_{total}}{(\text{cat}S\text{-denom})^2} + \dfrac{k_{RS}[\text{cat}R]_{total}[\text{cat}S]_{total}}{(\text{cat}R\text{-denom})(\text{cat}S\text{-denom})}}{\dfrac{k_S[\text{cat}S]^2_{total}}{(\text{cat}R\text{-denom})^2} + \dfrac{k_R[\text{cat}R]^2_{total}}{(\text{cat}R\text{-denom})^2} + \dfrac{k_{RS}[\text{cat}R]_{total}[\text{cat}S]_{total}}{(\text{cat}R\text{-denom})(\text{cat}S\text{-denom})}} \tag{22}$$

The simplest case of eq 22 where kinetic partitioning is negligible (cat*R*-denom and cat*S*-denom are equal to one or are equal to each other), gives eq 23. It may be shown that this case is mathematically equivalent to the ML_2 model or its DKEE analogy (eq 21) for dimeric catalysts when $K = 4$ (statistical distribution of species), although the physical meaning is different.

$$\frac{d[R]}{d[S]} = \frac{k_R[\text{cat}R]^2_{total} + k_S[\text{cat}S]^2_{total} + k_{RS}[\text{cat}R]_{total}[\text{cat}S]_{total}}{k_S[\text{cat}R]^2_{total} + k_R[\text{cat}S]^2_{total} + k_{RS}[\text{cat}R]_{total}[\text{cat}S]_{total}}\cdot\frac{f[R]}{f[S]} = k_{rel}\cdot\frac{f[R]}{f[S]} \tag{23}$$

Figure 8 shows experimental data from ref 4 for the kinetic resolution of racemic 1-pentene oxide plotted as DKEE versus ee$_{cat}$. These data are compared with the best fit of from the mechanism in Scheme 3 (eq 23, solid line) and with a standard ML_2 model as developed by Johnson and Singleton (eq 21, dashed line). The model based in Scheme 3 correctly predicts the trend of a positive nonlinear effect, but it cannot account for the magnitude of the experimentally observed asymmetric amplification. As mentioned above, the catalyst distribution in this model is constrained at $K = 4$ and the best fit gives $k_{RS} = 0$; inclusion of any contribution from the mixed catalyst pathways further *suppresses* rather than enhances the asymmetric amplification. By contrast, eq 21 does not constrain the catalyst distribution at $K = 4$ and, with two adjustable parameters instead of one, gives a better fit to the experimental data ($K = 129$ and $g = 0.12$). However, the mechanistic picture of Scheme 3 suggests that such an ML_2 model fit may not be physically meaningful.

A combination of the concept of kinetic partitioning together with the nonlinear effect due to the statistical distribution of catalyst interactions may give a more meaningful rationalization of the observed asymmetric amplification. This is in fact the case represented by eq 22, where it may be seen that the selectivity factor k_{rel} can vary with conversion. Indeed, Johnson and Singleton noted that the selectivity factor increased with conversion for the kinetic resolution shown in Figure 8. They also found that resolutions carried out in diffierent solvents gave different DKEE values as a function of ee_{cat}. They concluded from this that “the nonlinear effect must be treated as a separate variable, apart from the reaction’s asymmetric selectivity.” An alternate explanation might be that the binding constants for various species appearing in the denominators in eq 22 are themselves solvent-dependent, giving the possibility of different conversion-dependent “kinetic partitioning” effects in different solvents. As was discussed in the previous section, kinetic partitioning may be superimposed upon a nonlinear effect due to catalyst interactions to give a greater asymmetric amplification. In this case kinetic partitioning might help to explain why the observed asymmetric amplification is greater than that predicted from the statistical distribution of catalyst species. This suggests that the observed nonlinearity in the hydrolytic kinetic resolution could be a direct consequence of the reaction’s intrinsic kinetic properties, rather than a separate and independent variable.

Practical Implications of Kinetic Partitioning

Comparative Evaluation of Kinetic Partitioning and Classic Nonlinear Effects. Investigation of the selectivity factor as a function of conversion in kinetic resolutions using enantioimpure catalysts may help to differentiate between possible causes of anomalous selectivity behavior in cases where asymmetric amplification or depletion is observed. Classic nonlinear effects of catalyst aggregation may be inferred as the cause when the selectivity factor is found to be independent of conversion. For cases where a conversion dependence of k_{rel} is observed, a combination of classic nonlinear effects and kinetic partitioning will be implicated when anomalous selectivity behavior is observed even in the limit of very low conversion. Kinetic partitioning alone may be considered to be the cause if the selectivity factor at the low conversion limit is that given by the regular laws derived in refs 2 and 3 (eq 13 for the reaction network described in this paper) for noninteracting catalysts.

Mechanistic Considerations of Kinetic Partitioning. The parallel reaction networks which characterize kinetic resolutions make mechanistic studies of these reactions difficult. As in any complex catalytic reaction, detailed kinetic studies using enantiopure catalysts and enantiopure substrates would help to deconvolute the system by establishing the full reaction rate law for a proposed mechanism. Such studies have rarely been carried out in kinetic resolutions, and indeed in many cases investigations involving the enantiopure substrates are not practical. The concept of kinetic partitioning outlined in this paper, coupled with the use of enantioimpure catalysts, can extract significant information about the mechanism of a kinetic resolution and provide clues about the differences between the competing reaction networks. This is valid both in the case where nonlinear effects due to catalyst aggregation are present and in the case where they are absent.

Equation 7 showed that the selectivity factor in a kinetic resolution depends on both equilibrium binding and rate constants for the simple mechanism presented in Scheme 1. In general, both of these factors will play a role in more complex catalytic cycles. However, deconvoluting these two factors experimentally is difficult in a kinetic resolution carried out using enantiopure catalysts. Studying the conversion dependence of the selectivity factor in kinetic resolutions employing enantioimpure catalysts in a kinetic resolution offers a means of obtaining information about binding and rate constants separately.[12]

If no conversion dependence of k_{rel} is observed in a kinetic resolution, this suggests that the difference in reactivity between the two substrates must come about for reasons other than a strong preference for one substrate to bind to the catalyst. Interpretation in this case may focus on other parameters, such as differences in the rate of the product formation step.

If a conversion dependence of k_{rel} is observed, the direction of the trend with conversion can help to assess if the kinetic partitioning is beneficial (as for example, in the case shown in Figure 1a) or detrimental (Figure 1b) to the efficiency of the kinetic resolution. This information may in turn be used to inform strategies for improved catalyst design that seek to alter the substrate binding strengths in an appropriate manner.

Thus testing for a conversion dependence of the selectivity factor using enantioimpure catalysts provides a practical diagnostic of the origin of the rate difference between two enantiomeric substrates in a kinetic resolution and can aid in the rational design of catalysts. Such experiments could become a valuable standard practice in future studies of kinetic resolutions, even when the reactions will ultimately be carried out using enantiopure catalysts.

Conclusions

It has been demonstrated that the selectivity factor in kinetic resolutions carried out using enantioimpure catalysts may become a function of conversion due to “kinetic partitioning” of catalyst species within a complex reaction network. Thus, an additional mechanism for asymmetric amplification in kinetic resolutions has been identified which exists alone or may be superimposed on a classical nonlinear effect due to catalyst aggregation. Consideration of this behavior in kinetic resolutions using enantioimpure catalysts is of broad relevance since it may also provide fundamental mechanistic insight for improved practical application of kinetic resolutions which employ enantiopure catalysts.

Acknowledgment. D.G.B. gratefully acknowledges an unrestricted research grant from Pfizer Central Research and tutoring in Visual Basic programming from Professor P. D. I. Fletcher.

Supporting Information Available: Description of the Visual Basic programming for simulation of kinetic resolutions (PDF). This material is available free of charge via the Internet at http://pubs.acs.org.

JA002562O

---

(12) Accurate experimental measurement of selectivity factors is not trivial. Conversion and enantioselectivity are usually obtained in separate measurements, which increases the potential error. In addition, it is crucial to ensure that the enantioselectivity of the starting material is known at the beginning of the reaction. Selectivity factors will be observed to vary with conversion if eq 2 is used and the mixture of enantiomers is not truly racemic. The general equation given below may be more appropriate: $k_{rel} = \ln([R]/[R_o])/\ln([S]/[S_o])$